

Quantum circuit for three-qubit random states

Olivier Giraud,^{1,2} Marko Žnidarič,³ and Bertrand Georgeot^{1,2}

¹*Université de Toulouse; UPS; Laboratoire de Physique Théorique (IRSAMC); F-31062 Toulouse, France*

²*CNRS; LPT (IRSAMC); F-31062 Toulouse, France*

³*Department of Physics, Faculty of Mathematics and Physics, University of Ljubljana, SI-1000 Ljubljana, Slovenia*

(Received 24 March 2009; published 15 October 2009)

We explicitly construct a quantum circuit, which exactly generates random three-qubit states. The optimal circuit consists of three CNOT gates and fifteen single-qubit elementary rotations, parametrized by fourteen independent angles. The explicit distribution of these angles is derived, showing that the joint distribution is a product of independent distributions of individual angles apart from four angles.

DOI: [10.1103/PhysRevA.80.042309](https://doi.org/10.1103/PhysRevA.80.042309)

PACS number(s): 03.67.Ac, 03.67.Bg

I. INTRODUCTION

Quantum information science (see e.g., [1] and references therein) has received an increased attention in recent years due to the understanding that it enables to perform procedures not possible by purely classical resources. Experimental techniques to manipulate increasingly complex quantum systems are also rapidly progressing. One of the central issues is on the one hand to control and manipulate delicate complex quantum states in an efficient manner, but on the other hand at the same time to prevent all uncontrollable influences from the environment. In order to tackle such problems, one has to understand the structure and properties of quantum states. This can be done either through studies of particular states in a particular setting, or through focusing on the properties of the most generic states.

Random quantum states, that is states distributed according to the unitarily invariant Fubini-Study measure, are good candidates for describing generic states. Indeed, they are typical in the sense that statistical properties of states from a given Hilbert space are well described by those of random quantum states. Also, they describe eigenstates of sufficiently complex quantum systems [2] as well as time evolved states after sufficiently long evolution. Not least, because random quantum states possess a large amount of entanglement they are useful in certain quantum information processes such as quantum dense coding and remote state preparation [3,4]. Random unitary transformations on the other hand are employed e.g., in noise estimation [5] and twirling operations [6]. Sampling random states rather than random unitaries should also allow to obtain noise estimation protocols using a modification of the procedure in [5], while the use of random states in order to perform twirling would require development of new algorithms. An additional advantage of random states is that they are closely connected to the unitarily invariant Haar measure of unitary matrices, and the unitary invariance makes theoretical treatment of such states simpler.

Producing random states therefore enables to make available a useful quantum resource, and in addition to span the space of quantum states in a well-defined sense. Therefore several works have recently explored different procedure to achieve this goal. It is known that generating random states distributed according to the exact invariant measure requires a number of gates exponential in the number of qubits. A

more efficient but approximate way to generate random states uses pseudo-random circuits, in which gates are randomly drawn from a universal set of gates. As the number of applied gates increases the resulting measure gets increasingly close to the asymptotic invariant measure [7]. Some bipartite properties of random states can be reproduced in a number of steps that is smaller than exponential in the number of qubits. Polynomial convergence bounds have been derived analytically for bipartite entanglement [8–10] for a number of pseudorandom protocols. On the numerical side, different properties of circuits generating random states have been studied [11]. In order to quantify how well a given pseudorandom scheme reproduces the unitarily invariant distribution, one can study averages of low-order polynomials in matrix elements [12]. In particular, one can define a state (respectively, unitary) k -design, being a set of states (respectively, unitary matrices), for which moments up to order k agree with the average over Haar distribution [13,14]. Although exact state k -designs can be built for all k (see references in [14]) they are in general inefficient. In contrast, efficient approximate state k -designs can be constructed for arbitrary k [14] (for the specific case of an approximate unitary two-design see [9]).

The pseudorandom circuit approach can yield only pseudorandom states, which do not reproduce exactly the unitarily invariant distribution. The method has been shown to be useful for large number of qubits, where exact methods are clearly inefficient. However, for systems with few qubits, the question of asymptotic complexity is not relevant. It is thus of interest to study specifically these systems and to find the most efficient way—in terms of number of gates—to generate random states distributed according to the unitarily invariant measure. This question is not just of academic interest since, as mentioned, few-qubit random unitaries are needed for various quantum protocols. Optimal circuits for small number of qubits could also be used as a basic building block of pseudorandom circuits for larger number qubits, which might lead to faster convergence. In addition, systems of few qubits are becoming available experimentally, and it is important to propose algorithms that could be implemented on such small quantum processors, and which use as little quantum gates as possible. Indeed, quantum gates, and especially two-qubit gates, are a scarce resource in real systems, which should be carefully optimized.

Experimental realizations often rely on direct implementations of the quantum gates appearing in the circuit decom-

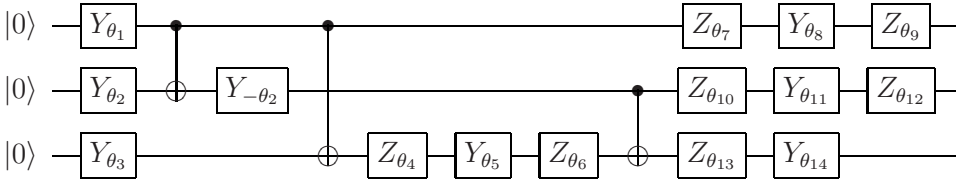


FIG. 1. Circuit \mathcal{C} for three-qubit random state generation.

position of the algorithm, applied on physical objects which are qubits or logical qubits. This usually requires to carefully optimize the number of one-qubit and two-qubit gates. One of the most widely used two-qubit gate is the controlled not (CNOT) gate, which together with one-qubit gates forms an universal set [15]. The CNOT gate is defined by its action on the computational basis $|00\rangle \rightarrow |00\rangle$, $|01\rangle \rightarrow |01\rangle$, $|10\rangle \rightarrow |11\rangle$, and $|11\rangle \rightarrow |10\rangle$. The CNOT gate (or the equivalent controlled phase flip) has been recently experimentally implemented using e.g., atom-photon interaction in cavities [16], linear optics [17], superconducting qubits [18,19] or ion traps [20,21]. It is clear from these experimental results that in general two-qubit gates such as the CNOT create much more decoherence than one-qubit gates. Thus, it appears that to adapt a quantum algorithm to existing experimental setups, one should limit as much as possible the number of such two-qubit gates. We note that three-qubit entangled states have already been realized and manipulated with ion traps [22,23], photons [24], and superconducting qubits [25].

In this paper, we therefore follow a different strategy from the more generally adopted approach of using pseudorandom circuits to generate pseudorandom states, and try and construct exact algorithms generating random states for systems of three qubits. In the language of k -designs such algorithms are exact ∞ -designs. Here, we present a circuit composed of one-qubit and two-qubit gates which produces exact random states in an optimal way, in the sense of using the smallest possible number of CNOT gates. The circuit uses in total three CNOT gates and 15 one-qubit elementary rotations. Our procedure uses results recently obtained [26] which described optimal procedures to transform a three-qubit state into another. Our circuit needs 14 random numbers, which should be classically drawn and used as parameters for performing the one-qubit gates. The probability distribution of these parameters is derived, showing that it factorizes into a product of 10 independent distributions of one parameter and a joint distribution of the 4 remaining ones, each of these distributions being explicitly given. Since we had to devise specific methods to compute these distributions, we explain the derivation in some details, as these methods can be useful in other contexts.

After presenting the main idea of the calculation in Sec. II, we start by treating the simple case of two-qubit states in Sec. III. We then turn to the three-qubit case and first show factorization of the probability distribution for a certain subset of the parameters (Sec. IV), the remaining parameters being treated in Sec. V. The full probability distribution for three qubits is summarized in Sec. VI.

II. QUANTUM CIRCUIT

Formally, a quantum state $|\psi\rangle$ can be considered as an element of the complex projective space $\mathbb{C}\mathbb{P}^{N-1}$, with $N=2^n$

the Hilbert space dimension for n qubits [27]. The natural Riemannian metric on $\mathbb{C}\mathbb{P}^{N-1}$ is the Fubini-Study metric, induced by the unitarily invariant Haar measure on $U(N)$. It is the only metric invariant under unitary transformations. While Haar measure is invariant under left and right unitary translation, the metric induced on the space of quantum states is invariant under left unitary translation only. To parametrize $\mathbb{C}\mathbb{P}^{N-1}$ one needs $2N-1$ independent real parameters. Such parametrizations are well known, for instance using Hurwitz parametrization of $U(N)$ [28]. However, they do not easily translate into one and two qubit operations, as desired in quantum information. In Ref. [26], optimal quantum circuits transforming the three-qubit state $|000\rangle$ into an arbitrary quantum state were discussed. In the case of three qubits, a generic state can be parametrized up to a global phase by 14 parameters. The quantum circuit requiring the smallest amount of CNOT gates has three CNOT gates and 15 one-qubit gates depending on 14 independent rotation angles. Indeed, it was shown in [26] that the set of pure quantum states of three qubits can be divided into four sets according to the minimal number of CNOT gates (0, 1, 2 or 3 gates) required to construct them from $|000\rangle$, disregarding the number of one-qubit gates. It turns out that almost all states belong to the last class requiring optimally three CNOTs. From [26] it is possible (see Appendix) to extract the circuit depicted in Fig. 1, expressed as a series of CNOT gates and single qubit rotations, where Z -rotation is $Z_\theta = \exp(-i\sigma_z\theta)$ and Y -rotation is $Y_\theta = \exp(-i\sigma_y\theta)$ with $\sigma_{y,z}$ the Pauli matrices. The circuit allows to go from $|000\rangle$ to any quantum state (up to an irrelevant global phase). It therefore provides a parametrization of a quantum state $|\psi\rangle$ by angles $\theta_1, \dots, \theta_{14}$.

In order to generate random vectors distributed according to the Fubini-Study measure, it would of course be possible to use e. g., Hurwitz parametrization to generate classically a random state, and then use the procedure described in [26] to find out the consecutive steps that allow to construct this particular vector from $|000\rangle$. However, this procedure requires application of a specific algorithm for each realization of the random vector. Instead, our aim here is to directly find the distribution of the θ_i such that the resulting $|\psi\rangle$ is distributed according to the Fubini-Study measure. This is equivalent to calculating the invariant measure associated with the parametrization provided by Fig. 1 in terms of the angles $\theta_1, \dots, \theta_{14}$. Geometrically, the Fubini-Study distance D_{FS} is the angle between two states $|\phi\rangle$ and $|\psi\rangle$,

$$\cos(D_{\text{FS}}) = \sqrt{\frac{\langle\phi|\psi\rangle\langle\psi|\phi\rangle}{\langle\phi|\phi\rangle\langle\psi|\psi\rangle}}. \quad (1)$$

The metric induced by this distance is obtained by taking $|\phi\rangle = |\psi\rangle + |d\psi\rangle$, getting

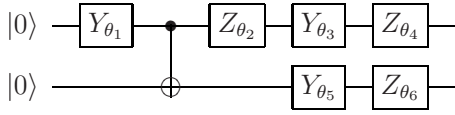


FIG. 2. Circuit for two-qubit random state generation.

$$ds^2 = \frac{\langle \psi | \psi \rangle \langle d\psi | d\psi \rangle - \langle \psi | d\psi \rangle \langle d\psi | \psi \rangle}{\langle \psi | \psi \rangle^2}, \quad (2)$$

where $\langle | \rangle$ is the usual Hermitian scalar product on C^n [29]. If a state $|\psi\rangle$ is parametrized by some parameters $\theta_1, \theta_2, \dots$ then the Riemannian metric tensor g_{ij} is such that $ds^2 = \sum g_{ij} d\theta_i d\theta_j$ and the volume form at each point of the coordinate patch, directly giving the invariant measure, is then given by $dv = \sqrt{\det(g)} \prod d\theta_i$ [30]. Thus, the joint distribution $P(\boldsymbol{\theta})$ of the θ_i is simply obtained by calculating the determinant of the metric tensor given by Eq. (2) with the parametrization $|\psi\rangle = |\psi(\boldsymbol{\theta})\rangle$, $\boldsymbol{\theta} = (\theta_1, \dots, \theta_{14})$. Unfortunately, the calculation of such a 14×14 determinant for $n=3$ qubits is intractable and one has to resort to other means. Let us first consider the easier cases of $n=1$ and 2 qubits, where by contrast the calculation can be performed directly.

III. SIMPLE EXAMPLES: ONE- AND TWO-QUBIT CASES

A normalized one-qubit state $|\psi\rangle = \cos \theta |0\rangle + e^{i\varphi} \sin \theta |1\rangle$ depends on two real angles θ, φ . It can be produced (up to a global phase) from the state $|0\rangle$ by application of the one-qubit gate $Y(\theta)$ followed by $Z(\varphi/2)$. The metric ds^2 can be easily calculated from Eq. (2) to be $ds^2 = d\theta^2 + \sin^2 \theta \cos^2 \theta d\varphi^2$. The matrix g is thus given by $g_{12} = g_{21} = 0$, $g_{11} = 1$, and $g_{22} = \sin^2 \theta \cos^2 \theta$, which implies that the angle distribution is given by $P(\theta, \varphi) = |\sin \theta \cos \theta|$. This distribution was derived e.g., in [31].

A normalized random two-qubit state $|\psi\rangle$ depends, up to a global phase, on 6 independent real parameters. A circuit producing $|\psi\rangle$ from an initial state $|00\rangle$ is depicted in Fig. 2. One can easily calculate the parametrization of the final state $|\psi(\theta_1, \dots, \theta_6)\rangle$ in terms of all six angles, thus directly obtaining the metric tensor g_{ij} from Eq. (2). Square root of the determinant of g then gives an unnormalized probability distribution of the angles as

$$P(\boldsymbol{\theta}) = |\cos^2 2\theta_1 \cdot \sin 2\theta_1 \cdot \sin 2\theta_3 \cdot \sin 2\theta_5| \quad (3)$$

(see also [32]). Several observations can be made about this distribution. First, the three rotations applied on the first qubit (top wire in Fig. 2) after the CNOT gate represent a random $SU(2)$ rotation, for which the Y -rotation angle is distributed as $P(\theta_3) \sim |\sin 2\theta_3|$ and the Z -rotation angles are uniformly distributed [28]. A similar argument holds for rotations on the second qubit. Second, angle θ_1 gives the eigenvalue of the reduced density matrix, $\lambda = \sin^2 \theta_1$, for which the distribution is well known, see, e.g., [31]. The third observation is that, remarkably, the joint distribution Eq. (3) of all 6 angles factorizes into six independent one-angle distributions.

IV. FACTORIZATION OF THE THREE-QUBIT DISTRIBUTION FOR ANGLES θ_7 TO θ_{14}

Let us now turn to our main issue, which is the distribution of angles in the three-qubit case. In order to have an indication whether the distribution of an angle θ_i also factorizes in this case, we numerically computed the determinant $\det(g)$ of the metric tensor as a function of θ_i with the other angles fixed. We also numerically computed the marginal distribution of θ_i by using the procedure given in the appendix to find the angles corresponding to a sample of uniformly distributed random vectors. If the distribution for a given angle θ_i factorizes, these two numerically computed functions should match (up to a constant factor). This is what we observed for all angles but four of them (angles θ_3 to θ_6).

In order to turn this numerical observation into a rigorous proof, we are going to show in this section that the distributions for angles θ_7 to θ_{14} indeed factorize. In the next section we will complete the proof by dealing with the cases θ_1 to θ_6 . The explicit analytical expression of the probability distribution for individual angles will be given in Sec. VI.

Let us denote by \mathcal{C} the circuit of Fig. 1 and by $C(\boldsymbol{\theta})$ the unitary operator corresponding to it, so that $|\psi(\boldsymbol{\theta})\rangle = C(\boldsymbol{\theta})|000\rangle$. Because circuits \mathcal{C} span the whole space of three-qubit states, any unitary three-qubit transformation V maps parameters $\boldsymbol{\theta}$ to new parameters $\tilde{\boldsymbol{\theta}}$ such that $V|\psi(\boldsymbol{\theta})\rangle = |\psi(\tilde{\boldsymbol{\theta}})\rangle$. We denote by $\tilde{\mathcal{C}}$ the circuit parametrized by angles $\tilde{\boldsymbol{\theta}}$ corresponding to performing \mathcal{C} followed by V . It is associated with the unitary operator $C(\tilde{\boldsymbol{\theta}})$ such that $C(\tilde{\boldsymbol{\theta}})|000\rangle = VC(\boldsymbol{\theta})|000\rangle$. Unitary invariance of the measure implies for $P(\boldsymbol{\theta})$ that

$$P(\boldsymbol{\theta}) = P(\tilde{\boldsymbol{\theta}}) |\mathcal{J}|, \quad (4)$$

with \mathcal{J} the Jacobian of the transformation $\boldsymbol{\theta} \rightarrow \tilde{\boldsymbol{\theta}}$ and $|\cdot|$ denotes the determinant. Note that Eq. (4) is not a simple change of variables, as the same function P appears on both sides of the equation. The Jacobian matrix \mathcal{J} for transformation V from angles $\boldsymbol{\theta}$ to $\tilde{\boldsymbol{\theta}}$, $V|\psi(\boldsymbol{\theta})\rangle = |\psi(\tilde{\boldsymbol{\theta}})\rangle$, tells how much do the angles $\tilde{\boldsymbol{\theta}}$ of $|\psi(\tilde{\boldsymbol{\theta}})\rangle$ change if we vary angles $\boldsymbol{\theta}$ in $|\psi(\boldsymbol{\theta})\rangle$ keeping transformation matrix V fixed. Choosing V that sets some angles θ_j in circuit $\tilde{\mathcal{C}}$ to a fixed value, say zero, and at the same time showing that $|\mathcal{J}|$ depends only on these angles θ_j , would prove factorization of $P(\boldsymbol{\theta})$ with respect to angles θ_j through Eq. (4).

A. Gates 7–12 and 14

The simplest case is that of gates at the end of the circuit \mathcal{C} of Fig. 1, e.g., gate θ_{14} . For V we take Y -rotation by angle $-u$ on the third qubit, $V = Y_{-u}$. It defines a mapping $\boldsymbol{\theta} \rightarrow \tilde{\boldsymbol{\theta}}$ such that $\tilde{\theta}_i = \theta_i$ for $i \leq 13$ and $\tilde{\theta}_{14} = \theta_{14} - u$. Matrix elements of the Jacobian, i.e., partial derivatives $\mathcal{J}_{jk} = \partial \tilde{\theta}_j / \partial \theta_k$, are equal to δ_{jk} . The Jacobian is equal to an identity matrix and its determinant is one. Equation (4) taken at $u = \theta_{14}$ then gives $P(\theta_1, \dots, \theta_{13}, 0) = P(\theta_1, \dots, \theta_{13}, \theta_{14})$, from which one concludes that the distribution for θ_{14} factorizes and is in fact uniform (unless noted otherwise P 's are not normalized).

The same argument holds for the two other rotations by angles θ_{12} and θ_9 applied at the end of each qubit wire.

Proceeding to angle θ_8 one could use $V=Y_{-u_8}Z_{-u_9}$ applied on the first qubit and show that the Jacobian depends only on θ_8 and θ_9 , while at $u_8=\theta_8$ and $u_9=\theta_9$ one gets $\tilde{\theta}_8=\tilde{\theta}_9=0$, from which factorization of θ_8 would follow from Eq. (4). There is however a simpler way. Observe that the three single-qubit gates with angles θ_7 , θ_8 and θ_9 on the first qubit span the whole $SU(2)$ group. Therefore, for any one-qubit unitary V , gates $VZ_{\theta_9}Y_{\theta_8}Z_{\theta_7}$ can be rewritten as $Z_{\tilde{\theta}_9}Y_{\tilde{\theta}_8}Z_{\tilde{\theta}_7}$, without affecting other θ 's. The distribution of these three angles must therefore be the same as the distribution of corresponding $SU(2)$ parameters. Note that the same argument can be applied for two-qubits in Fig. 2. As a consequence, the distribution of angles for gates Z - Y - Z at the end of the circuit should be the same in both cases, that is the distribution of θ_7 is uniform while that of θ_8 is proportional to $|\sin 2\theta_8|$. Similarly, one can show that the distribution for the angles θ_{10} to θ_{12} is the same as for angles θ_7 to θ_9 .

B. Gate 13

As opposed to gates 10–12, for gate 13 we cannot use the analogy with the two-qubit circuit (Fig. 2) because the two gates 13 and 14 on the third qubit are not in the same order as they were in the two-qubit circuit. Gate 13 is thus, a more difficult one.

Using $V=Z_{-u_{13}}Y_{-u_{14}}$ on the third qubit, we can set $\tilde{\theta}_{13}$ and $\tilde{\theta}_{14}$ to zero with the choice $u_{13}=\theta_{13}$ and $u_{14}=\theta_{14}$. Our goal is to show that $|\mathcal{J}|$ depends only on θ_{13} and θ_{14} . We can formally consider each angle $\tilde{\theta}_i$ as being a function $\tilde{\theta}_i(\boldsymbol{\theta}; u_{13}, u_{14})$ of the initial $\boldsymbol{\theta}$ as well as of the parameters $u_{13,14}$ through $C(\tilde{\boldsymbol{\theta}}|000)=VC(\boldsymbol{\theta}|000)$. To calculate matrix elements of \mathcal{J} for our choice of V evaluated at $u_{13}=\theta_{13}$ and $u_{14}=\theta_{14}$, we must obtain the first-order expansion in ϵ of the quantities

$$\tilde{\theta}_j(\theta_1, \dots, \theta_{k-1}, \theta_k + \epsilon, \theta_{k+1}, \dots, \theta_{14}; \theta_{13}, \theta_{14}). \quad (5)$$

Some angles $\tilde{\theta}_j$ are easy to calculate. We immediately see that varying angles $\theta_{j \leq 12}$, which is taking $k \leq 12$ in Eq. (5), angles $\tilde{\theta}_{j \leq 12}$ do not change. The corresponding 12×12 -dimensional sub-block in \mathcal{J} is therefore equal to an identity matrix. Similarly, varying θ_{13} we see that $\tilde{\theta}_{j \leq 13}$ do not change. The corresponding column in \mathcal{J} is therefore zero apart from 1 on the diagonal. The Jacobian thus, has a block structure of the form

$$|\mathcal{J}| = \begin{vmatrix} \mathbb{1} & B \\ 0 & A \end{vmatrix} = |A|, \quad (6)$$

where $\mathbb{1}$ is a 13×13 -dimensional identity matrix and A is a 1×1 -dimensional block with partial derivative $\partial \tilde{\theta}_{14} / \partial \theta_{14}$. The angle $\tilde{\theta}_{14}$ given by Eq. (5) is obtained by varying angle θ_{14} by ϵ .

Angles $\tilde{\theta}_j$ in Eq. (5) for $k=14$ are determined from the condition $C(\tilde{\boldsymbol{\theta}}|000)=VC(\boldsymbol{\theta}|000)$. In the following we are

going to find angles $\tilde{\boldsymbol{\theta}}$, in particular, we are going to give explicit expressions for $\tilde{\theta}_{13,14}$ in terms of $\theta_{13,14}$ to the lowest order in ϵ . To this aim, we will exhibit a particular set of angles $\tilde{\boldsymbol{\theta}}$ which verifies $C(\tilde{\boldsymbol{\theta}}|000)=VC(\boldsymbol{\theta}|000)$ at first order in ϵ and therefore should coincide at first order with the exact solution which is known to exist from the Appendix.

Because angles θ_{7-12} appear in the circuit after gates θ_{13} and θ_{14} , the gates involving θ_{7-12} commute with V and thus, we can choose $\tilde{\theta}_j=\theta_j$ for $7 \leq j \leq 12$. The corresponding gates simplify on both sides of the equation $C(\tilde{\boldsymbol{\theta}}|000)=VC(\boldsymbol{\theta}|000)$, and thus the state $C(\boldsymbol{\theta}|000)$ after this simplification can be written as

$$|\psi\rangle = \cos \theta_1 |00\rangle U_A U_B |\gamma\rangle + \sin \theta_1 |1\rangle (\sin 2\theta_2 |0\rangle U_A + \cos 2\theta_2 |1\rangle U_A \sigma_x) U_B \sigma_x |\gamma\rangle, \quad (7)$$

where we use short notation for the third qubit, $|\gamma\rangle = \cos \theta_3 |0\rangle + \sin \theta_3 |1\rangle$, $U_A = Y_{\theta_{14+\epsilon}} Z_{\theta_{13}}$ are the two gates acting on the third qubit after the last CNOT and $U_B = Z_{\theta_6} Y_{\theta_5} Z_{\theta_4}$ are the three gates before the last CNOT. If we choose $\tilde{\theta}_{1-3} = \theta_{1-3}$, then identifying the three orthogonal terms in Eq. (7) obtained from $C(\tilde{\boldsymbol{\theta}}|000)$ and from $VC(\boldsymbol{\theta}|000)$, we must have three equalities between states on the third qubit:

$$U'_A U_B |\gamma\rangle = \tilde{U}_A \tilde{U}_B |\gamma\rangle,$$

$$U'_A U_B \sigma_x |\gamma\rangle = \tilde{U}_A \tilde{U}_B \sigma_x |\gamma\rangle,$$

$$U'_A \sigma_x U_B \sigma_x |\gamma\rangle = \tilde{U}_A \sigma_x \tilde{U}_B \sigma_x |\gamma\rangle, \quad (8)$$

where \tilde{U}_A and \tilde{U}_B are the same as U_A and U_B but with $\tilde{\boldsymbol{\theta}}$ instead of $\boldsymbol{\theta}$ (note that $\theta_{14+\epsilon} \rightarrow \tilde{\theta}_{14}$), and $U'_A := V U_A = Z_{-\theta_{13}} Y_{\epsilon} Z_{\theta_{13}}$. These three equations can actually be solved using two matrix equations, namely, $U'_A U_B = \tilde{U}_A \tilde{U}_B$ and $U'_A \sigma_x U_B = \tilde{U}_A \sigma_x \tilde{U}_B$. If these two matrix equations are satisfied, the above three state equalities Eq. (8) are automatically fulfilled. To find a solution one first eliminates $\tilde{U}_B = U_A^{-1} U'_A U_B$ to obtain a single matrix equation $U'_A \sigma_x U_A^{-1} = \tilde{U}_A \sigma_x \tilde{U}_A^{-1}$. Writing out matrix elements explicitly one gets two equations for the new angles $\tilde{\theta}_{13}$ and $\tilde{\theta}_{14}$,

$$\cos 2\theta_{13} \sin 2\epsilon = \cos 2\tilde{\theta}_{13} \sin 2\tilde{\theta}_{14},$$

$$\cos^2 \epsilon - (\sin^2 \epsilon e^{4i\theta_{13}}) = (\cos^2 \tilde{\theta}_{14} e^{-2i\tilde{\theta}_{13}}) - (\sin^2 \tilde{\theta}_{14} e^{2i\tilde{\theta}_{13}}). \quad (9)$$

Solving these two equations to the lowest order in ϵ one gets $\tilde{\theta}_{14} = \epsilon \cos 2\theta_{13} + o(\epsilon^2)$ and $\tilde{\theta}_{13} = 0 + o(\epsilon^2)$. Once we have $\tilde{\theta}_{13}$ and $\tilde{\theta}_{14}$ one can get angles $\tilde{\theta}_{4-6}$ from $\tilde{U}_B = \tilde{U}_A^{-1} U'_A U_B$. Because the three angles in \tilde{U}_B span (up to a global phase) the whole set of one-qubit transformations, one can always find suitable $\tilde{\theta}_{4-6}$. Since we have produced a solution $\tilde{\boldsymbol{\theta}}$, which is the correct one up to first order in ϵ , we can conclude that the derivative $\partial \tilde{\theta}_{14} / \partial \theta_{14}$ is equal to $\cos 2\theta_{13}$ and thus is independent of angles $\theta_1, \dots, \theta_6$. This completes the proof that the

distribution for θ_{13} factorizes. Incidentally, we also see that the distribution of θ_{13} is proportional to $|\cos 2\theta_{13}|$.

V. JOINT THREE-QUBIT PROBABILITY DISTRIBUTION FOR ANGLES θ_1 TO θ_6

In the preceding section, we have shown that the distribution for angles θ_7 to θ_{14} factorizes. As was mentioned, numerical observations indicated us that the distribution for angles θ_1 and θ_2 should also factorize, but that it is not the case for the joint distribution of $\theta_3, \dots, \theta_6$.

As we were not able to directly prove by the same methods as above that the distributions for θ_1 and θ_2 factorize, we use a different strategy. Namely, we first assume that this factorization is true, then we compute the distributions under this assumption, and the knowledge of the answer allows us to prove *a posteriori* that it is indeed the correct probability distribution.

If the factorization holds, the distribution for θ_1 and θ_2 is easily calculated from the matrix g using symbolic manipulation software, by replacing angles $\theta_j, j \geq 3$, in g by suitably chosen simple values, so that the 14×14 determinant giving the volume form can now be handled. This yields, up to a normalization constant,

$$P_1(\theta_1) = \cos^5 \theta_1 \sin^9 \theta_1 \quad (10)$$

$$P_2(\theta_2) = \cos^5 2\theta_2 \sin^3 2\theta_2. \quad (11)$$

The joint distribution of $\theta_3, \dots, \theta_6$ cannot be further factorized, and requires heavy calculations. Indeed, even replacing all angles but $\theta_3, \dots, \theta_6$ by numerical values the determinant $\det(g)$ of the metric tensor given by Eq. (2) still depends on 4 variables, which is too much for it to be evaluated by standard software. We thus proceeded as follows. First one can show that $\det(g)$ can be put under the form

$$\det(g) = \sum_{p=-10}^{10} \sum_{q=-6}^6 \sum_{r=-8}^8 \sum_{s=-6}^6 a_{pqrs} \cos(2p\theta_3 + 2q\theta_4 + 2r\theta_5 + 2s\theta_6), \quad (12)$$

with the sums running over all q, r but only even values of p and s . Indeed, each coefficient of the matrix g is a trigonometric polynomial whose degree in each variable can be calculated. Replacing coefficients by monomials and expanding the determinant gives an upper bound on the degree of the trigonometric polynomial $\det(g)$. Because of the parity of \cos , there are $M=8509$ independent coefficients a_{pqrs} . Evaluating numerically the determinant at M random values of the angles one gets an $M \times M$ linear system that can be solved numerically. If the values of the coefficients of the matrix g_{ij} are multiplied by a factor 4, then one is ensured [from inspection of $\det(g)$] that the a_{pqrs} are rationals of the form $k/2^9, k \in \mathbb{Z}$. This allows to deduce their exact value from the numerical result. We are left with 6998 nonzero terms in $\det(g)$, and terms with odd q or r do not exist. We then suppose that $\sqrt{\det(g)}$ can be expanded as

$$\sqrt{\det(g)} = \sum_{p=-5}^5 \sum_{q=-3}^3 \sum_{r=-4}^4 \sum_{s=-3}^3 b_{pqrs} e^{i(2p\theta_3 + 2q\theta_4 + 2r\theta_5 + 2s\theta_6)}. \quad (13)$$

This assumption is validated *a posteriori*, since a solution of the form Eq. (13) can indeed be found. There are 4851 coefficients b_{pqrs} , which can be obtained by identifying term by term coefficients in the expansion of $[\sqrt{\det(g)}]^2$ and $\det(g)$. We have to solve a system of quadratic equations

$$\begin{aligned} a_{10,6,8,6} &= b_{5343}^2 \\ a_{10,6,8,5} &= b_{5342}b_{5343} + b_{5343}b_{5342} \\ a_{10,6,8,4} &= b_{5341}b_{5343} + b_{5342}b_{5342} + b_{5343}b_{5341} \\ &\dots = \dots \end{aligned} \quad (14)$$

The first equation is quadratic and fixes an overall sign. Equation $k+1$ is linear once the values obtained from the first k equations are plugged into it. Starting with the highest-degree term $(p, q, r, s) = (5, 3, 4, 3)$ one can thus recursively solve all equations. There are only 1320 nonzero coefficients b_{pqrs} . Gathering together terms $(\pm p, \pm q, \pm r, \pm s)$ one can simplify the sum Eq. (13) to a sum of 96 terms of the form $c_{pqrs} \cos(p\theta_3) \cos(q\theta_4) \cos(r\theta_5) \sin(s\theta_6)$. Expanding this expression in powers of $\cos(2\theta_5)$ and $\sin(2\theta_5)$ and simplifying separately each coefficient we finally get

$$P(\theta_3, \theta_4, \theta_5, \theta_6) = \sin 2\theta_5 \sin 4\theta_3 \sin^2 \varphi_1 \cos \varphi_2, \quad (15)$$

where $\langle \alpha | \bar{\beta} \rangle = \cos \varphi_1$ and $\langle \beta | \bar{\beta} \rangle = \cos \varphi_2$ with $|\alpha\rangle = U_B |\gamma\rangle$, $|\beta\rangle = U_B \sigma_x |\gamma\rangle$ (see Sec. IV B). Recall that $|\bar{\beta}\rangle$ is the bit-flip transform of $|\beta\rangle$, $|\bar{\beta}\rangle = \sigma_x |\beta\rangle$. Note that $\sin 2\theta_3 = \langle \alpha | \beta \rangle$. Angles $\varphi_{1,2}$ can be obtained from

$$\begin{aligned} \cos^2 \varphi_1 &= (c_4 c_5 c_6 - s_4 s_6)^2 + (c_3 c_4 s_6 + c_3 s_4 c_5 c_6)^2 \\ \cos \varphi_2 &= -s_3 s_4 s_6 + c_6 (s_3 c_4 c_5 - c_3 s_5), \end{aligned} \quad (16)$$

where $c_i = \cos 2\theta_i$ and $s_i = \sin 2\theta_i$. We do not have a general argument to explain this remarkable expression of the distribution in terms of the scalar products of $|\alpha\rangle$, $|\beta\rangle$ and $|\bar{\beta}\rangle$.

To complete the proof for the joint distribution $P(\theta_1, \dots, \theta_6)$ it remains to be checked that the determinant of the metric tensor g with angles θ_7 to θ_{14} replaced by constants is indeed equal to $P_1(\theta_1)P_2(\theta_2)P(\theta_3, \theta_4, \theta_5, \theta_6)$. This *a posteriori* verification is easier to handle symbolically than the full *a priori* calculation of the 14×14 determinant. Indeed, the determinant can first be reduced to an 8×8 determinant by Gauss-Jordan elimination. The remaining determinant can be expanded as a trigonometric polynomial. Although symbolic manipulation softwares do not allow to simplify the coefficients of this polynomial, they are able to check that these coefficients match those of the expected distribution. We proved in that way that the difference between the determinant $\det(g)$ and our expression is identically zero. This gives a computer assisted but rigorous proof for the distribution of angles θ_1 to θ_6 .

VI. TOTAL THREE-QUBIT PROBABILITY DISTRIBUTION FUNCTION

Gathering together the results of the previous sections we obtain that the joint distribution $P(\boldsymbol{\theta})$ can be factorized as

$$P(\boldsymbol{\theta}) = \left| P_1(\theta_1)P_2(\theta_2)P(\theta_3, \theta_4, \theta_5, \theta_6) \prod_{i=7}^{14} P_i(\theta_i) \right|. \quad (17)$$

The joint distribution $P(\theta_3, \theta_4, \theta_5, \theta_6)$ has been derived in the previous section and is given by Eq. (15). The distribution for θ_1 and θ_2 is given by Eqs. (10) and (11). Given the factorization Eq. (17), it is easy to calculate the remaining $P_i(\theta_i)$ for each $i=7, \dots, 14$ as was done for θ_1 and θ_2 in the previous section: replacing angles θ_j , $j \neq i$, in g by suitably chosen simple values, the 14×14 determinant giving the volume form can be easily evaluated by standard symbolic manipulation. This yields, up to a normalization constant,

$$\prod_{i=7}^{14} P_i(\theta_i) = \sin 2\theta_8 \sin 2\theta_{11} \cos 2\theta_{13}. \quad (18)$$

The knowledge of the angle distribution Eq. (17) allows to easily generate random three-qubit vectors using the circuit of Fig. 1. Angles θ_1 , θ_2 , and θ_7 to θ_{14} can be drawn classically according to their individual probability distribution. Angles $\theta_3, \dots, \theta_6$ can be obtained classically from the joint distribution Eq. (15) by, for instance, Monte-Carlo rejection method (that is, drawing angles θ_3 to θ_6 and a parameter $x \in [0, p]$ at random, and keeping them if $P(\theta_3, \theta_4, \theta_5, \theta_6) < x$). Bounding $P(\theta_3, \theta_4, \theta_5, \theta_6)$ from above by $p=0.85$ yields a success rate of about 12%.

VII. CONCLUSION

In this work, we constructed a quantum circuit for generating three-qubit states distributed according to the unitarily invariant measure. The construction is exact and optimal in the sense of having the smallest possible number of CNOT gates. The procedure requires a set of 14 random numbers classically drawn, which will be the angles of the one-qubit rotations, and whose distribution has been explicitly given. Remarkably, we have shown that the distribution of angles factorizes, apart from that of four angles. The circuit can be used as a three-qubit random state generator, thus producing at will typical states on three qubits. It could be also used as a building block for pseudo-random circuits in order to produce pseudorandom quantum states on an arbitrary number of qubits, e.g., using repeated applications of our circuit on subsets of three qubits. At last, it gives an example of a quantum algorithm producing interesting results which could be implemented on a few-qubit platform, using only 18 quantum gates, of which 15 are one-qubit elementary rotations much less demanding experimentally.

ACKNOWLEDGMENTS

We thank the French ANR (Project No. INFOSYSQQ) and the IST-FET program of the EC (Project No. EUROS-

QIP) for funding. M.Ž. would like to acknowledge support by Slovenian Research Agency, Grant No. J1-7437, and hospitality of Laboratoire de Physique Théorique, Toulouse, where this work has been started.

APPENDIX: THE PARAMETRIZATION OF FIG. 1

In this Appendix, we explain how to obtain the angles θ_i of the circuit (Fig. 1) for a given $|\psi\rangle$, based on the discussion in [26]. This justifies the use of these angles as a parametrization of the quantum states. We start from a state $|\psi\rangle$, and transform it by the inverse of the different gates of Fig. 1 to end up with $|000\rangle$, specifying how the angles θ_i are obtained in turn. More details can be found in [26]. Any three-qubit state $|\psi\rangle$ can be written in a canonical form as a sum of two (not normalized) product terms [33],

$$|\psi\rangle = |\omega_1\omega_2\omega_3\rangle + |\omega_1^\perp\rangle|\xi\rangle_{23}, \quad (A1)$$

where $|\omega_i\rangle$ are one-qubit states, $|\omega_1^\perp\rangle$ is a one-qubit state orthogonal to $|\omega_1\rangle$ and $|\xi\rangle_{23}$ is a two-qubit state of the second and third qubits. The angle θ_9 is chosen such that the Z-rotation of angle $-\theta_9$ eliminates a relative phase between the coefficients of the expansion of $|\omega_1\rangle$ into $|0\rangle$ and $|1\rangle$. (Note that because we are using the circuit in the reverse direction the angles of rotations have opposite signs). A subsequent Y rotation with angle $-\theta_8$ results in the transformation $|\omega_1\rangle \rightarrow |0\rangle$ (up to a global phase). Similarly, rotations of angles $-\theta_{12}$ and $-\theta_{11}$ rotate $|\omega_2\rangle$ into $|0\rangle$. After applying rotations of angles $-\theta_8$, $-\theta_9$, $-\theta_{11}$, and $-\theta_{12}$ the state has become of the form $|\psi'\rangle = |00\gamma\rangle + |1\rangle(|0\gamma_1\rangle + |1\gamma_2\rangle)$ (up to normalization). Two rotations on the third qubit of angles $-\theta_{13}$ and $-\theta_{14}$ are now chosen so as to rotate $|\gamma_1\rangle$ into some new state $|\gamma'\rangle$ while $|\gamma_2\rangle$ is rotated, up to normalization, into $\sigma_x|\gamma'\rangle$. It was shown in [26] that this can always be done by writing the normalized $|\gamma_{1,2}\rangle$ as $|\gamma_{1,2}\rangle = \cos \phi_{1,2}|0\rangle + e^{i\xi_{1,2}} \sin \phi_{1,2}|1\rangle$, and then θ_{14} is a solution of

$$-\tan(2\theta_{14}) = \frac{\cos 2\phi_1 + \cos 2\phi_2}{\sin 2\phi_1 \cos \xi_1 + \sin 2\phi_2 \cos \xi_2}, \quad (A2)$$

while $\theta_{13} = -(\delta_1 + \delta_2)/4$, where δ 's are relative phases in $Y_{-\theta_{14}}|\gamma_{1,2}\rangle = e^{i\delta_{1,2}} \cos \kappa|0\rangle + \sin \kappa|1\rangle$. Acting with a CNOT₂₃ gate on the resulting state one obtains a quantum state for the three qubits of the form $|\psi''\rangle = |00\chi_1\rangle + |1\omega_4\chi_2\rangle$, with $\chi_2 = \gamma'$. The Z-rotation angle $-\theta_{10}$ on the second qubit is now determined so as to eliminate a relative phase between the expansion coefficients of $|\omega_4\rangle$, making them real up to a global phase. On the third qubit we now apply three rotations of angles $-\theta_4$, $-\theta_5$, and $-\theta_6$ to bring $|\chi_1\rangle$ to $|\chi'\rangle$ and $|\chi_2\rangle$ into $\sigma_x|\chi'\rangle$, eliminating also a relative phase. Then a CNOT₁₃ gate is applied. At this point (after the second CNOT gate in Fig. 1, counting from right, but without the θ_7 rotation), the state has become of the form $|\psi'''\rangle = \cos \theta_1|00\omega_6\rangle + e^{i\tau} \sin \theta_1|1\omega_5\omega_6\rangle$, where the one-qubit states $|\omega_5\rangle$ and $|\omega_6\rangle$ are normalized and real. With θ_7 we now eliminate the relative phase τ , and with an Y-rotation of angle $-\theta_3$ the third qubit is brought to the state $|0\rangle$. Then the combination of two Y-rotation of angles

θ_2 and $-\theta_2$ with a CNOT_{12} gate brings the second qubit to $|0\rangle$, and the last rotation of angle $-\theta_1$ on the first qubit yields the final state $|000\rangle$. Note that in the circuit of Fig. 1 the two Z-rotations of angles θ_7 and θ_{10} commute with CNOT gates if

they act on the control qubit. This is the reason why the rotation of angle θ_7 can be applied at any point between θ_1 and θ_8 and, similarly, θ_{10} can be applied at any point between θ_2 and θ_{11} .

-
- [1] M. A. Nielsen and I. L. Chuang, *Quantum Computation and Quantum Information* (Cambridge, Cambridge, 2000).
- [2] F. Haake, *Quantum Signatures of Chaos*, 2nd ed. (Springer Verlag, Berlin, 2001).
- [3] A. Harrow, P. Hayden, and D. Leung, Phys. Rev. Lett. **92**, 187901 (2004); A. Abeyesinghe *et al.*, IEEE Trans. Inf. Theory **52**, 3635 (2006).
- [4] P. Hayden, D. Leung, P. W. Shor, and A. Winter, Commun. Math. Phys. **250**, 371 (2004); C. H. Bennett *et al.*, IEEE Trans. Inf. Theory **51**, 56 (2005); A. Ambainis and A. Smith, Lect. Notes Comput. Sci. **3122**, 249 (2004).
- [5] J. Emerson, R. Alicki, and K. Życzkowski, J. Opt. B: Quantum Semiclassical Opt. **7**, S347 (2005); B. Levi, C. C. Lopez, J. Emerson, and D. G. Cory, Phys. Rev. A **75**, 022314 (2007).
- [6] G. Toth and J. J. Garcia-Ripoll, Phys. Rev. A **75**, 042311 (2007).
- [7] J. Emerson, Y. S. Weinstein, M. Saraceno, S. Lloyd, and D. G. Cory, Science **302**, 2098 (2003).
- [8] R. Oliveira, O. C. O. Dahlsten, and M. B. Plenio, Phys. Rev. Lett. **98**, 130502 (2007); O. C. O. Dahlsten, R. Oliveira, and M. B. Plenio, J. Phys. A **40**, 8081 (2007).
- [9] A. W. Harrow and R. A. Low, Commun. Math. Phys. **291**, 257 (2009).
- [10] M. Žnidarič, Phys. Rev. A **78**, 032324 (2008).
- [11] Y. S. Weinstein and C. S. Hellberg, Phys. Rev. Lett. **95**, 030501 (2005); M. Žnidarič, Phys. Rev. A **76**, 012318 (2007); Y. Most, Y. Shimoni, and O. Biham, *ibid.* **76**, 022328 (2007); D. Rossini and G. Benenti, Phys. Rev. Lett. **100**, 060501 (2008); Y. S. Weinstein, W. G. Brown, and L. Viola, Phys. Rev. A **78**, 052332 (2008); L. Arnaud and D. Braun, *ibid.* **78**, 062329 (2008).
- [12] J. Emerson, E. Livine and S. Lloyd, Phys. Rev. A **72**, 060302(R) (2005).
- [13] C. Dankert, R. Cleve, J. Emerson, and E. Livine, e-print arXiv:quant-ph/0606161.
- [14] A. Ambainis and J. Emerson, in *Proceedings of the XXII Annual Conference on Computational Complexity* (IEEE Computer Society, Los Alamitos, CA, 2007), pp. 129–140.
- [15] A. Barenco, C. H. Bennett, R. Cleve, D. P. DiVincenzo, N. Margolus, P. Shor, T. Sleator, J. A. Smolin, and H. Weinfurter, Phys. Rev. A **52**, 3457 (1995).
- [16] A. Rauschenbeutel, G. Noguez, S. Osnaghi, P. Bertet, M. Brune, J. M. Raimond, and S. Haroche, Phys. Rev. Lett. **83**, 5166 (1999).
- [17] J. L. O’Brien, G. J. Pryde, A. G. White, T. C. Ralph, and D. Branning, Nature (London) **426**, 264 (2003); S. Gasparoni, J.-W. Pan, P. Walther, T. Rudolph, and A. Zeilinger, Phys. Rev. Lett. **93**, 020504 (2004).
- [18] T. Yamamoto, Yu. A. Pashkin, O. Astafiev, Y. Nakamura, and J. S. Tsai, Nature (London) **425**, 941 (2003).
- [19] J. H. Plantenberg, P. C. de Groot, C. J. P. M. Harmans, and J. E. Mooij, Nature (London) **447**, 836 (2007).
- [20] D. Leibfried, B. DeMarco, V. Meyer, D. Lucas, M. Barrett, J. Britton, W. M. Itano, B. Jelenković, C. Langer, T. Rosenband, and D. J. Wineland, Nature (London) **422**, 412 (2003).
- [21] M. Riebe, K. Kim, P. Schindler, T. Monz, P. O. Schmidt, T. K. Körber, W. Hänsel, H. Häffner, C. F. Roos, and R. Blatt, Phys. Rev. Lett. **97**, 220407 (2006).
- [22] D. Leibfried, M. D. Barrett, T. Schaetz, J. Britton, J. Chiaverini, W. M. Itano, J. D. Jost, C. Langer, and D. J. Wineland, Science **304**, 1476 (2004).
- [23] C. F. Roos, M. Riebe, H. Häffner, W. Hänsel, J. Benhelm, G. P. T. Lancaster, C. Becher, F. Schmidt-Kaler, and R. Blatt, Science **304**, 1478 (2004).
- [24] M. Eibl, N. Kiesel, M. Bourennane, Ch. Kurtsiefer, and H. Weinfurter, Phys. Rev. Lett. **92**, 077901 (2004).
- [25] J. M. Fink, R. Bianchetti, M. Baur, M. Goeppl, L. Steffen, S. Filipp, P. J. Leek, A. Blais, and A. Wallraff, Phys. Rev. Lett. **103**, 083601 (2009).
- [26] M. Žnidarič, O. Giraud, and B. Georgeot, Phys. Rev. A **77**, 032320 (2008).
- [27] I. Bengtsson and K. Życzkowski, *Geometry of Quantum States* (Cambridge University Press, Cambridge, 2006).
- [28] A. Hurwitz, Nachr. Ges. Wiss. Goettingen, Math.-Phys. Kl. **1**, 71 (1897).
- [29] V. I. Arnold, *Mathematical Methods of Classical Mechanics, Graduate Texts in Mathematics* (Springer, New York, 1978).
- [30] T. Frankel, *The Geometry of Physics—An Introduction* (Cambridge University Press, Cambridge, 1997).
- [31] K. Życzkowski and H.-J. Sommers, J. Phys. A **34**, 7111 (2001).
- [32] I. Bengtsson, J. Braennlund, and K. Życzkowski, Int. J. Mod. Phys. A **17**, 4675 (2002).
- [33] A. Acín, A. Andrianov, L. Costa, E. Jané, J. I. Latorre, and R. Tarrach, Phys. Rev. Lett. **85**, 1560 (2000).